



ELSEVIER

Available online at www.sciencedirect.com

 ScienceDirect

Solar Energy Materials
& Solar Cells

Solar Energy Materials & Solar Cells 90 (2006) 3531–3546

www.elsevier.com/locate/solmat

Photovoltaic activity of a PolyProDOT derivative in a bulk heterojunction solar cell

Luis M. Campos^{a,*}, Attila J. Mozer^b, Serap Günes^b,
Christoph Winder^b, Helmut Neugebauer^b, N. Serdar Sariciftci^b,
Barry C. Thompson^c, Benjamin D. Reeves^c, Christophe
R.G. Grenier^c, John R. Reynolds^c

^a*Department of Chemistry & Biochemistry and Exotic Materials Institute,
University of California, Los Angeles, CA 90095-1569, USA*

^b*Linz Institute for Organic Solar Cells (LIOS) Physical Chemistry, Johannes Kepler University Linz,
Altenbergerstrasse 69, A-4040 Linz, Austria*

^c*The George and Josephine Butler Polymer Research Laboratory, Department of Chemistry and Center for
Macromolecular Science and Engineering, University of Florida, Gainesville, FL 32611-7200, USA*

Received 18 March 2006; received in revised form 13 June 2006; accepted 14 June 2006

Available online 17 August 2006

Abstract

We report the photophysical behavior and photovoltaic performance of a poly(3,4-propylenedioxythiophene) (PProDOT) derivative, namely poly-[3,3-dihexyl-3,4-dihydro-2H-thieno(3,4-b)(1,4)dioxepine] (PProDOT(Hx)₂), as an electron donor in bulk heterojunction solar cells blended with the acceptor 1-(3-methoxycarbonyl)propyl-1-phenyl-[6,6]-methanofullerene (PCBM). Devices composed of a 1:4 (w:w) ratio of PProDOT(Hx)₂/PCBM and spin coated from chlorobenzene were characterized by measuring current–voltage characteristics under simulated Air Mass 1.5 (AM1.5) conditions as well as the spectrally resolved photocurrent (IPCE). The influence of different preparation parameters like various blend ratios, spin coating from different solvents, and changing the metal contacts was studied. It was found that the photoluminescence of the polymer is quenched by a factor greater than 100 using blends consisting of PProDOT(Hx)₂ and PCBM (3:2, w:w). Additionally, the photoactive blends were characterized by photoinduced absorption spectroscopy and the results suggest that charge transfer is occurring from PProDOT(Hx)₂ to PCBM. Results

*Corresponding author.

E-mail address: lcampos@chem.ucla.edu (L.M. Campos).

from atomic force microscopy reveal that a bicontinuous network, with domain sizes on the order of 100–200 nm, results when a 1:4 blend of PProDOT(Hx)₂/PCBM is spin coated from chlorobenzene. © 2006 Elsevier B.V. All rights reserved.

Keywords: Polymer solar cells; Multifunctional materials; Propylenedioxythiophene; PProDOT(Hx)₂; PCBM

1. Introduction

The discovery of photoinduced charge transfer from the excited state (π^*) of poly[2-methoxy-5-(2'-ethylhexyloxy)-1,4-phenylene vinylene] (MEH-PPV) to Buckminsterfullerene (C₆₀) [1] has triggered a broad search for organic materials to be introduced in the production of 'plastic' solar cells [2,3]. Solar cells based on the bulk heterojunction concept [4] have been predicted to reach efficiencies of 5% or greater using commercially available materials [5]. Bulk heterojunction solar cells are composed of intimately mixed p-type (electron donor) with n-type (electron acceptor) materials, yielding an active layer of nanoscale p–n junctions where the photoinduced charge transfer takes place [6]. The two most widely used donor polymers are PPV (poly(*p*-phenylene vinylene) derivatives such as MEH-PPV or poly[2-methoxy-5-(3'-7'-dimethyloxy)-1,4-phenylene vinylene] (MDMO-PPV), as well as polythiophene derivatives such as poly(3-hexylthiophene) (P3HT). The fullerene derivative 1-(3-methoxycarbonyl)propyl-1-phenyl-[6,6]-C₆₁ (PCBM) is the electron acceptor material most commonly used in the blends. The electron transfer in conjugated polymer-C₆₀ systems has been shown to be very efficient and in the sub-picosecond regime [7]. Consequently, the presence of small amounts of fullerene (and derivatives) can quench the photoluminescence (PL) by more than three orders of magnitude [8]. Devices using MDMO-PPV have reached efficiencies of approximately 3% [9], while the P3HT counterparts have been recently reported to yield nearly 5% [5].

In the ongoing attempt to maximize the efficiency of polymer-based photovoltaic devices, the interdisciplinary nature of the research effort has become a central theme. It is generally accepted that the realization of high efficiency (5–10%) plastic solar cells will stem from device optimization on several levels. From a physical or engineering standpoint, improvement of the device structure is critical, as the proper choice of electrode materials [10,11] as well as buffer layers [12], has a strong impact on the device characteristics. Additionally, improvement in device fabrication conditions can lead to the maximum efficiencies using available donor and acceptor materials [13]. However, from the materials point of view, new polymers are also a viable means of producing high-efficiency solar cells. New polymers offer a means of overcoming current device deficiencies by modifying the chemical structure of the polymer rather than the device architecture. Low-band gap polymers are especially attractive as they promise to increase the absorption of solar photons, especially near the peak of solar emission photon flux at 1.8 eV [14,15]. The synthesis of new organic polymers can also be tailored to fit specific demands based on structure–property relationships. For example, a major drawback of currently available semiconducting polymers is their relative instability [16]. Furthermore, polymers must be easily processable, soluble in common organic solvents, and available in gram amounts, among other demands. At the molecular level, it is imperative that the donor polymer can interact with the acceptor for charge transfer, and the polymer must exhibit good hole transport properties [14].

Focusing toward new polymer development, thiophene-based polymers such as P3HT, have great potential for application in photovoltaic devices. Their synthesis and band gap manipulation has been widely explored and is well understood [17]. One of the most successful polythiophenes in industry is poly(3,4-ethylenedioxythiophene) (PEDOT) [18,19]. Modification of the core structure of PEDOT has resulted in the design of numerous electrochemically polymerizable monomers displaying attractive features for use in electrochromic devices, such as a low oxidation potential stemming from the electron rich nature of the polymer backbone [20]. An important feature for electrochromics, transformation of the ethylenedioxy bridge found in PEDOT to the propylenedioxy bridge in poly(3,4-propylenedioxythiophene) (PProDOT) resulted in higher contrast ratios and faster switching speeds upon symmetrical disubstitution of the central carbon on the propylene bridge, as in the case of dimethyl-PProDOT (PProDOT(Me)₂) [21]. The incorporation of longer alkyl groups on these disubstituted PProDOT's facilitated the chemical synthesis of soluble polymers via the Grignard metathesis polymerization (GriM) [22]. As a result, we have developed a family a solution processable, spray-coatable PProDOT's [23] that have been successfully incorporated into electrochromic devices [24].

In this paper, we introduce the use of poly-(3,3-dihexyl-3,4-dihydro-2*H*-thieno[3,4-*b*][1,4]dioxepine) (PProDOT(Hx)₂) [23a] as an electron donor for photovoltaic devices. This dihexyl-substituted derivative of PProDOT has been synthesized on the gram scale with molecular weights of up to ~38,000 g/mol (M_n) and shows good solubility in numerous organic solvents such as toluene, dichloromethane, chloroform (CF), and THF. PProDOT(Hx)₂ is an excellent film-forming polymer that is capable of forming free-standing films of sufficient mechanical integrity for handling and cutting. The band gap of PProDOT(Hx)₂ is estimated to be 1.9 eV as measured from thin-film optical absorbance and the polymer shows a quantum efficiency for fluorescence of 0.50 in toluene solution. Based on its excellent processability and performance in electrochromic devices, PProDOT(Hx)₂ shows promising characteristics for use in multiple materials applications, such as photovoltaic devices and thin-film transistors. Here, we report the performance of a number of bulk heterojunction devices that have been prepared by blending PProDOT(Hx)₂ with PCBM.

2. Experimental

2.1. Materials

PProDOT(Hx)₂ was synthesized by a GriM as described previously [23a] The sample used in the present study was found to have $M_n = 27,500$ and $M_w = 47,600$ g/mol for a PDI = 1.73 (GPC, THF vs. polystyrene). Elemental analysis, calculated: C, 70.76; H, 9.40. Found: C, 68.03; H, 8.61. UV–Vis (toluene) $\lambda_{\max} = 585$ nm (2.5×10^4 l mol⁻¹ cm⁻¹). PCBM was provided by J.C. Hummelen from Rijksuniversiteit Groningen. PEDOT-PSS (Baytron PH PEKA, 3061443-10) was purchased from Bayer, AG.

2.2. UV–Vis absorption and photoluminescence (PL)

UV–Vis absorption spectra in solution and in solid thin films were obtained using a Hewlett-Packard 8453 spectrophotometer. Thin films for UV–Vis were spin coated on glass from chlorobenzene (CB) and CF solutions containing 3.5 mg of PProDOT(Hx)₂ in

1 ml of solvent, and varying ratios of PProDOT(Hx)₂:PCBM (w:w; 1:1, 1:2, 1:3, 1:4, respectively). PL and photoluminescence excitation (PLE) in solution was measured on a Hitachi F 4010 instrument in a rectangular geometry.

2.3. Photoinduced absorption (PIA)

Photoinduced absorption (PIA) spectra of solid films in the VIS/NIR were measured with a homemade setup at 80 K [25b]. The samples were excited by a mechanically chopped laser light with the 514 nm line of an Ar⁺ laser. The chopping frequency was typically 237 Hz, the laser power was approximately 40 mW on a spot size of 4 mm in diameter. A 120 W tungsten halogen lamp was used as a probe. The changes in the probe transmission, induced by the laser excitation, were detected by a modulation technique using a Stanford Research System, Model SR 830 DSP, lock-in amplifier. A Si–InGaAsSb sandwich detector with a set of gratings and filters was used to measure the spectra. The PL was measured separately by detecting the sample response on the pump without probe. The PIA spectra ($-dT/T \approx \alpha d$) were corrected for the luminescence of the sample normalized for the probe light transmission.

2.4. Atomic force microscopy (AFM)

The atomic force microscopy (AFM) studies were performed by using Digital Instruments Dimension 3100 in the tapping mode. Tapping-mode AFM operates by scanning a tip attached to the end of an oscillating cantilever across the sample surface. By maintaining a constant oscillation amplitude, a constant tip–sample interaction is maintained during imaging. Thin films for AFM characterization were spin coated on glass from different solvents.

2.5. Photovoltaic devices: fabrication

The overall layered structure of the devices is shown in Fig. 1. The indium tin oxide (ITO) coated glass was cleaned in an ultrasonic bath with acetone and isopropanol. An aqueous solution of poly(3,4-ethylenedioxythiophene)–poly(styrenesulfonate) (PEDOT:PSS) was spin coated on the glass–ITO substrate, and dried under a dynamic vacuum. The resulting PEDOT:PSS layer was approximately 100 nm thick. The PProDOT(Hx)₂:PCBM active layer was spin coated on top of the PEDOT:PSS layer using different solvents (CB, CF). The blends for the active layer contained a 1:1, 1:2, 1:3, or 1:4 (w:w) ratio of PProDOT(Hx)₂:PCBM, prepared by dissolving 3.5 mg of PProDOT(Hx)₂ and 14 mg of PCBM (in the case of 1:4)/ml of solvent, and stirring at 50 °C overnight in the dark in a sealed tube, under argon atmosphere. The thickness of the films ranged from 100 to 150 nm as measured by AFM. The top electrodes, LiF (0.6 nm, Aldrich) and Al (90–100 nm, Aldrich), were added by vapor deposition under low pressure ($< 10^{-5}$ mbar) using a shadow mask to achieve an area of 5 mm². Calcium–aluminum (30 nm/60 nm, Aldrich) contacts were also studied. All current–voltage (I – V) characteristics of the PV devices were measured (using a Keithley SMU 2400 unit) under inert-atmosphere conditions (argon) in a dry glove box immediately after production. A Steuernagel solar simulator, simulating AM1.5 conditions, was used as the excitation source with an input power of 100 mW cm⁻² white-light illumination. The PV devices made from the 1:4 blend

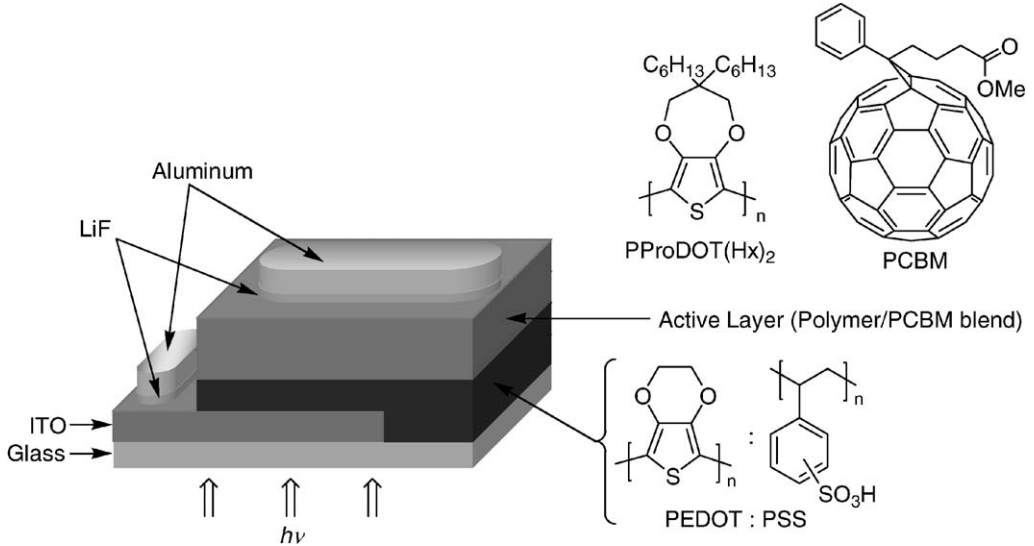


Fig. 1. Schematic representation of the layered bulk heterojunction solar cell and chemical structures corresponding to PProDOT(Hx)₂, PCBM, and PEDOT:PSS.

were treated under several post-production treatment conditions: (a) heating (H) at 85 °C for $t = 4$ min while applying a positive bias (B) of 2 V, (b) $H = 95$ °C, $t = 4$ min, $B = +2$ V, (c) $H = 105$ °C, $t = 4$ min, $B = +2$ V, (d) $H = 105$ °C, $t = 4$ min, $B = +3$ V, (e) $H = 115$ °C, $t = 4$ min, $B = +3$ V and (f) $H = 125$ °C, $t = 4$ min, $B = +2$ V.

The spectrally resolved photocurrent was measured with a EG&G Instruments 7260 lock-in amplifier. The samples were illuminated with monochromatic light from a Xenon lamp (FWHM ~ 4 nm, illumination density ranging between ~ 50 and $\sim 200 \mu\text{W cm}^{-2}$), chopped with a frequency of 273 Hz. The incident photon to current efficiency (% IPCE) was calculated according to Eq. (A1):

$$\text{IPCE}(\%) = \frac{I_{\text{sc}} \times 1240}{P_{\text{in}} \times \lambda_{\text{incident}}}, \quad (\text{A1})$$

where I_{sc} ($\mu\text{A cm}^{-2}$) is the measured current under short-circuit conditions of the solar cell, P_{in} (W m^{-2}) is the incident light power, measured with a calibrated silicon diode, and λ (nm) is the incident photon wavelength.

The evaluation of the solar cells was carried out by using the power conversion efficiency Eq. (A2).

$$\eta_{\text{AM1.5}}(\%) = \left(\frac{P_{\text{out}}}{P_{\text{in}}} \right) \times 100 = \frac{\text{FF} \times V_{\text{oc}} \times J_{\text{sc}}}{P_{\text{in}}} \times 100. \quad (\text{A2})$$

The percentage efficiency, $\eta_{\text{AM1.5}}$, is given by the ratio of the power output (P_{out}), to the power input from the solar simulator (P_{in} , 100 mW cm^{-2}). The output power of a solar cell under illumination is the product of the fill factor FF, the open-circuit voltage V_{oc} (V), and the current density under short-circuit conditions J_{sc} (mA cm^{-2}). The FF is obtained

from Eq. (A3).

$$FF = \frac{V_{\text{mpp}} \times J_{\text{mpp}}}{V_{\text{oc}} \times J_{\text{sc}}}, \quad (\text{A3})$$

where the maximum-power point of the product of the voltage and the current density (V_{mpp} , and J_{mpp}) is divided by the product of the open-circuit voltage and the short-circuit current [25].

3. Results and discussion

3.1. Photophysical properties of PProDOT(Hx)₂ and PProDOT(Hx)₂/PCBM blends

The highest occupied molecular orbital (HOMO)–lowest unoccupied molecular orbital (LUMO) levels (valence and conduction band onset energy) of PProDOT(Hx)₂ were determined electrochemically as described previously and illustrated schematically in Fig. 2 [23a] Using cyclic voltammetry, the HOMO was estimated at 5.05 eV (~ 5.1 eV), relative to vacuum assuming that the Fc/Fc⁺ redox couple is +0.380 V vs. saturated calomel electrode (SCE) [26], and that the SCE is poised 4.7 eV relative to vacuum [27] (which places Fc/Fc⁺ at ~ 5.1 eV relative to vacuum). The polymer was not found to exhibit a reversible reduction and thus the LUMO is estimated at ~ 3.2 eV based on the difference between the electrochemically measured HOMO and the optically determined band gap ($E_g = 1.9$ eV). As with all dioxythiophene polymers, the relatively low oxidation potential is the result of the electron-rich nature of the polymer backbone attributable to the donating nature of the ether functional groups. The band energies for PCBM were taken from the literature [23b]. It can be seen in Fig. 2 that the HOMO of PProDOT(Hx)₂ is higher in energy than that of MEH-PPV [28] and P3HT [29] by 0.3 and 0.4 eV, respectively (values for MEH-PPV and P3HT were corrected for Fc/Fc⁺ = 5.1 eV vs. vacuum). At the same time, the LUMO of PProDOT(Hx)₂ provides a sufficient offset of ~ 1.0 eV (similar to

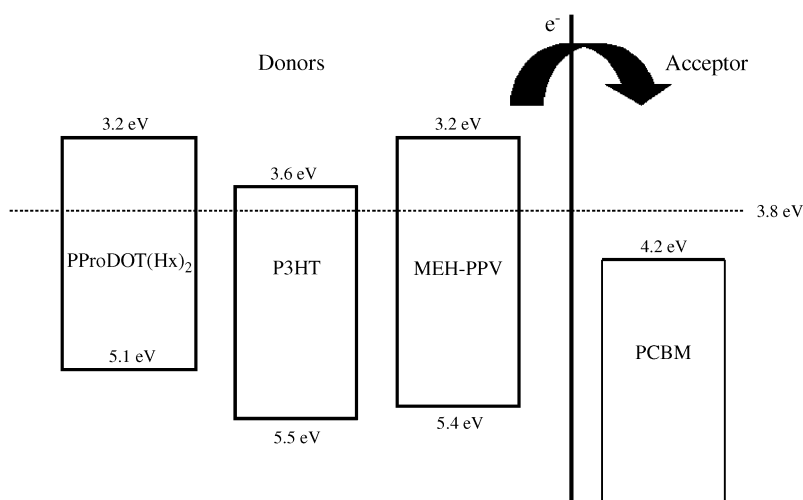


Fig. 2. Energy-level diagrams for PProDOT(Hx)₂, P3HT, and MEH-PPV relative to PCBM. The dashed line indicates the minimum donor LUMO energy required for effective charge transfer to PCBM (~ 3.8 eV).

MEH-PPV) relative to the LUMO of PCBM. This energy offset is far more than the requisite minimum of 0.3–0.4 eV [30,31], which is generally believed to be necessary to ensure effective charge transfer from the photoexcited polymer to PCBM.

The UV–Vis absorbance and PL spectra of PProDOT(Hx)₂ solutions and thin films are shown in Fig. 3. The lowest energy electronic transition in solution (solid line) is relatively broad, ranging from 425 to 625 nm, with a λ_{\max} at 585 nm and a smaller peak at 545 nm. The polymer solution exhibits a deep red luminescence with an emission maximum at 610 nm and a less-intense transition at 665 nm. Both the absorbance and PLE mission spectra of PProDOT(Hx)₂ show more vibronic resolution than other substituted polythiophenes (PTs) reported by Theander et al. [32], who suggested the formation of aggregates. Furthermore, such previously reported PTs exhibit larger Stokes shifts in the order of 90–100 nm. Our polymer has a very small Stokes shift of 25 nm, suggesting that the polymer does not aggregate or has large structural relaxations upon excitation but, the co-planarity of the thiophene units may be affected. It has been proposed that aggregation effects in solution may cause the PL to show signs of excimer-like emission, i.e., the shift of the emission should be greater than that of a conformational change along the coplanar backbone [33–35]. The small Stokes shift is an indication that the polymer is rigid and does not necessarily aggregate, possibly due to the two hexyl chains in the propylene bridge, which branch orthogonal to the polythiophene backbone and increase the solubility of the polymer.

In thin films, the UV–Vis absorption and PLE spectra (dashed lines) are relatively similar to those obtained in solution (Fig. 3), and only small changes can be observed. The higher energy absorption at 545 nm is more intense than the 585 nm band in the UV–Vis spectrum of the film. Nonetheless, both absorption spectra retain a similar shape regardless of the medium. The PL spectrum in the solid film is slightly red-shifted by 12 nm (λ_{\max} at 622 nm) relative to that in solution, and shows a redistribution of intensities. The emission band at 675 nm and the smaller shoulder at 740 nm are more pronounced, relative to the corresponding emission bands in solution. Such spectral characteristics can be

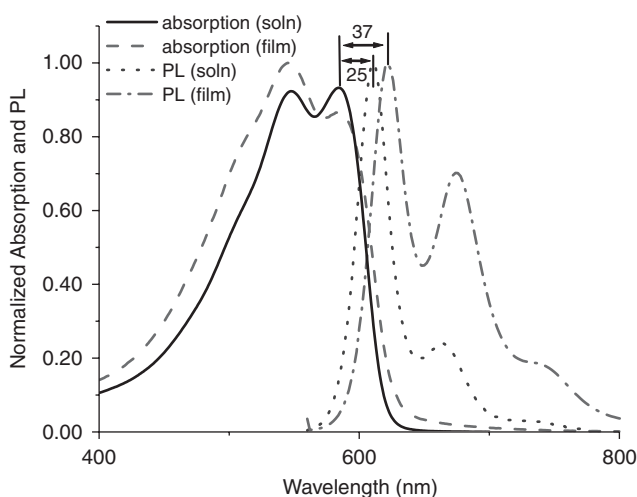


Fig. 3. Plot of the UV–Vis absorption (solid; solution; dash, film), and the (PL, after excitation at 540 nm; dot, solution; dash-dot, film) of pristine PProDOT(Hx)₂ in toluene solution at room temperature and thin film.

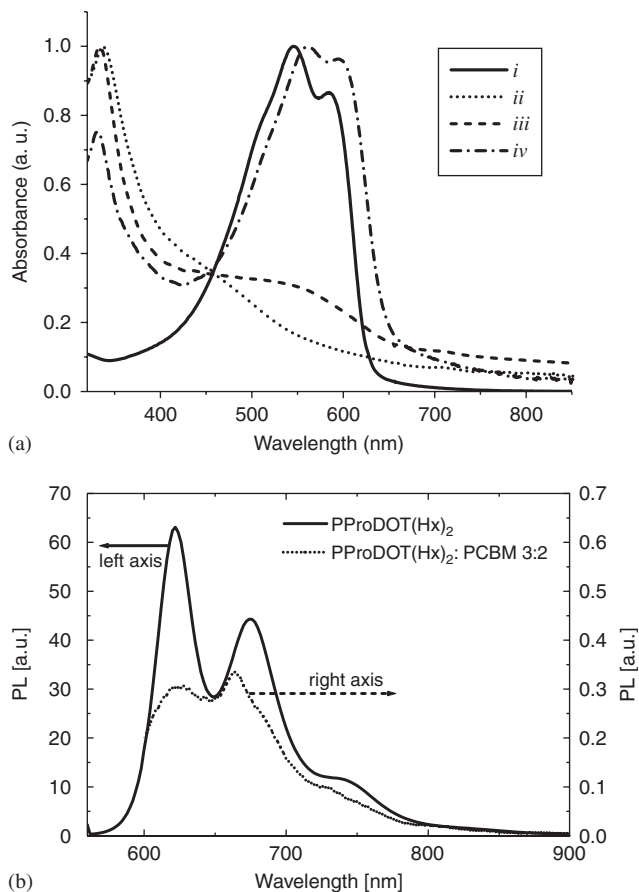


Fig. 4. (a) Normalized UV-Vis spectra of pristine PProDOT(Hx)₂ (i, solid line), pristine PCBM (ii, short-dot line), PProDOT(Hx)₂ (0.35%)/PCBM blend (1:4, w:w; iii, short-dash line), and PProDOT(Hx)₂ (0.35%)/PCBM blend (3:2, w:w; iv, short-dash-dot line); all were thin-films spin coated from CB. (b) PL emission, after 514 nm excitation, of pristine PProDOT(Hx)₂ (left axis) and PProDOT(Hx)₂/PCBM (3:2, w:w; right axis).

attributed to the planarization and increased rigidity of the conjugated system of PProDOT(Hx)₂ in films, as it has been previously observed for smaller conjugated molecules [33,36]. Changes in the medium can affect the conformational dynamics and the equilibrium population of conjugated systems. Therefore, certain absorbance and emission transitions can be enhanced, diminished, and/or shifted [35].

Upon blending PProDOT(Hx)₂ with PCBM, the UV-Vis spectrum broadens and loses some vibronic resolution (Fig. 4a). The 330 nm band in the blends corresponds to PCBM, as it can be seen from the pristine PCBM absorption spectrum. Furthermore, Fig. 4b shows that the PL is quenched in the PProDOT(Hx)₂/PCBM blend (3:2, w:w) by a factor greater than 100. The PL of both the pristine polymer and the blend was measured after excitation at 514 nm. Although PL quenching is not a conclusive proof of a charge transfer mechanism, it shows evidence of the interaction between PProDOT(Hx)₂ and PCBM. In this case, the polymer is postulated to act as an electron donor following the photoinduced excitation. This is supported by the proposed band structure for PProDOT(Hx)₂ in Fig. 2

and the fact that PCBM is known to be an electron acceptor [37], favoring the charge transfer mechanism [38].

Fig. 5 shows the photocurrent action spectrum obtained from the 1:4 polymer/PCBM blend spin coated from CB. The % IPCE plot exhibits a maximum photocurrent contribution of 7.4% at 445 nm and a smaller peak at 345 nm that may correspond to the contribution from PCBM (Fig. 5), which has an absorption at 330 nm (Fig. 4a). It is apparent that the photoinduced charge transfer is active over a relatively wide range of wavelengths, 300–620 nm, as is expected for a device containing a polymer with a low band gap of 1.9 eV. The % IPCE is used to obtain information on the energy of the photons that contribute to the current generation in the solar cell [2]. Correlation of the % IPCE to the photon absorption spectrum can be categorized as symbiotic when both the absorbance spectrum matches the IPCE, and antibatic for spectra that do not match [39]. While the IPCE does show a small shoulder between 550 and 600 nm, the maximum at 445 nm does not correspond to any feature in the absorption spectrum of the blend. Thus, Fig. 5 clearly shows a mismatch of the plots. Such behavior has been attributed to an internal filter effect, which is characteristic of current generation only near the electrode collecting the less mobile charge, resulting in a shift of the maximum peak to balance the amount of light absorbed and the region of the light absorption [40,41]. It has also been shown that in donor–acceptor blends, where the concentration of the acceptor is high, the charge transfer is the rate-limiting step but separation of the electron–hole pairs is the more important for the efficiency of the PV device [42].

To better understand the charge transfer process taking place in these blends, PIA spectra were obtained. The PIA spectrum of pristine PProDOT(Hx)₂ film shows a maximum peak at approximately 1.23 eV (Fig. 6). The features around 1.8–1.9 eV are probably residual uncompensated PL, which is much stronger in this energy range than the PIA. The modulation frequency dependence at the peak wavelength is weak in the range between 4 and 4000 Hz, no lifetime can be calculated. Additionally, the dependence of the

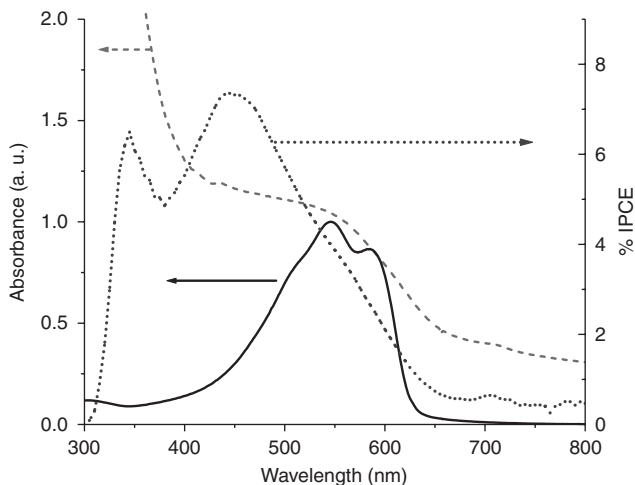


Fig. 5. Photon absorbance plot of pristine PProDOT(Hx)₂ (solid line, left axis) and PProDOT(Hx)₂/PCBM (1:4, w:w) blend (dashed line, left axis), in addition to the % IPCE plot of the PProDOT(Hx)₂/PCBM (1:4, w:w) blend (dotted line, right axis).

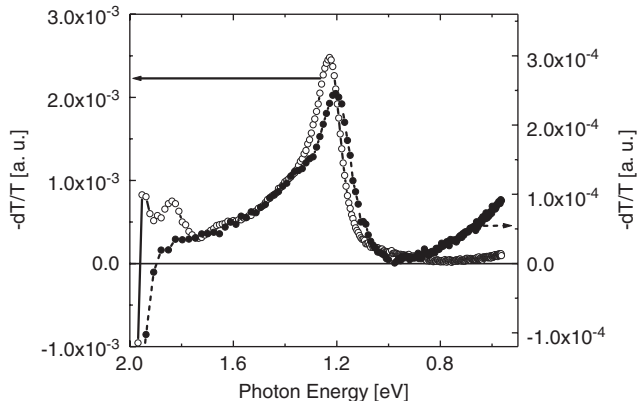


Fig. 6. PIA of pristine PProDOT(Hx)₂ (full line, open circles) and a PProDOT(Hx)₂/PCBM blend (3:2, w:w ratio, dashed line, full circles). PIA was measured at 77 K with excitation at 514 nm and 40 mW. The intensity of the transmitted light is given by T .

PIA signal upon increasing the laser pump power, I , shows a power law dependence I^k , with $k = 0.75$ and therefore, cannot be clearly assigned to either first-order or second-order decay kinetics. Photobleaching of the ground state absorption is observed above 1.9 eV. The onset for the bleaching can be used to estimate the band gap and the value of 1.9 eV (650 nm) is in good agreement with the ground state absorption onset. The PIA of the PProDOT(Hx)₂/PCBM blend shows an absorption feature between 1 and 2 eV, with a peak at 1.2 eV, as well as a second absorption arising below 0.6 eV. The modulation frequency dependence for the two features at 1.2 and 0.6 eV show similar behavior. A mean lifetime of $\tau = 0.7$ ms with a broad distribution is calculated ($\alpha = 0.55$) [43]. The pump power dependence shows a nearly square root dependence ($k = 0.47$), indicating a dominant second-order kinetic recombination.

In summary, for pristine films of PProDOT(Hx)₂, strong PL is observed, exhibiting a single PIA peak as found from the PIA measurements. Such PIA is commonly assigned to triplet-triplet absorption. After blending with the electron acceptor PCBM, the PL is quenched and two PIA peaks are observed. Such PIA spectra with two photoinduced transitions in the band gap, are commonly assigned to distributed polaronic charge carriers on a disordered conjugated polymer [14]. The broad distribution of lifetimes and the second-order kinetics of the decay confirm this assumption. The PL quenching and PIA results support a photoinduced charge transfer from PProDOT(Hx)₂ to PCBM.

3.2. Photovoltaic devices: performance

We have evaluated the performance of PProDOT(Hx)₂ as a possible electron donor material for incorporation in bulk heterojunction solar cells [2] with PCBM. The solar cells were optimized by varying several standard parameters. It has been shown that spin coating from different solvents [44,45], varying the polymer-to-PCBM ratio [46], changing the metal contacts [47], using PEDOT:PSS as a hole-contact layer [6], and post-production treatment [48], among other factors, can be used to optimize the efficiency of the devices. In summary, our observation was that the best PProDOT(Hx)₂-based bulk heterojunction

solar cell was composed of 0.35% PProDOT(Hx)₂ in CB and four equivalents (by weight) of PCBM. Using the device architecture shown in Fig. 1, these devices gave an efficiency of 0.1% under simulated AM1.5 conditions.

Solar cells composed of the pristine polymer in the active layer did not significantly generate photocurrent under illumination. The strong PL observed in the pristine polymer indicates that the excited state decays without charge generation. Additionally, the open-circuit voltage ($V_{oc} = 0.560$ V) was at its highest value, compared to all the devices that were prepared.

The I - V characteristic curves in the dark and under illumination of the PProDOT(Hx)₂/PCBM, 1:4 (w:w) blend are shown in Fig. 7. With the PProDOT(Hx)₂/PCBM devices, the open circuit voltage (V_{oc}) of the blend is lower than that of the pristine polymer by approximately 0.270 V. A similar drop in the V_{oc} of MDMO-PPV/PCBM devices has been observed, relative to the pristine MDMO-PPV device [46]. The FF of this device also plays an important role in the overall low efficiency of the cell, and thus the value of 0.38 observed here is indicative of the poor performance of these devices. In general, parallel and series resistances can account for the low FF. It has been shown that improving the charge transport of the donor polymer can increase the FF of solar cells (up to 0.7) [25]. It is interesting to note that this novel PProDOT derivative exhibits photovoltaic characteristics when blended with PCBM, in addition to electrochromism in pristine films [23a]. As an electrochromic material PProDOT(Hx)₂ is observed to reversibly change from a highly absorptive dark blue-purple to a transmissive sky blue upon electrochemical oxidation. Such multifunctional materials are potentially interesting and can perhaps ultimately be exploited to harness all of their properties in a device. While these films were deposited by spin coating, PProDOT(Hx)₂ can be efficiently coated onto the surfaces by other methods including spray coating which has been successfully employed in the development of electrochromic devices [23a].

We have also studied the effect of reducing the amount of PCBM in the active layer, but this failed to improve the efficiency of the solar cells. Devices containing

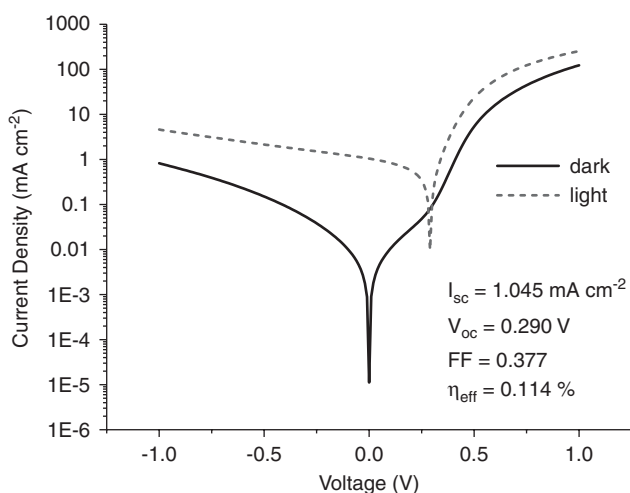


Fig. 7. Semilogarithmic plots of the current–voltage (I - V) characteristics of a PProDOT(Hx)₂/PCBM (1:4) solar cell, spin coated from CB (structure: glass-ITO/PEDOT:PSS/PProDOT(Hx)₂:PCBM (1:4)/LiF-Al).

Table 1

Photovoltaic properties of the PProDOT(Hx)₂-based bulk heterojunction solar cells using different ratios of PCBM

PProDOT(Hx) ₂ /PCBM ratio (w:w)	I_{sc} (mA cm ⁻²)	V_{oc} (V)	FF	η_{eff} (%) ^a
1:0	0.003	0.56	0.35	0.0007
1:1	0.23	0.32	0.36	0.03
1:2	0.49	0.31	0.34	0.05
1:3	0.80	0.27	0.33	0.07
1:4	1.05	0.29	0.38	0.11
1:4 ^b	0.81	0.30	0.38	0.09
1:4 ^c	0.89	0.28	0.38	0.09

I_{sc} = short-circuit current, V_{oc} = open-circuit voltage, FF = fill factor, η_{eff} = percentage conversion efficiency.

Unless otherwise noted, the active layer was spin coated from CB and the contacts used were LiF/Al.

^aUncorrected values.

^bUsing Ca/Al (30/60 nm) contacts.

^cSpin coated from CF.

PProDOT(Hx)₂:PCBM in ratios of 1:1, 1:2, and 1:3, respectively, were prepared (in addition to the 1:4 blend). The results are summarized in Table 1. We observed a decrease in the current density concomitant with the decrease of PCBM concentration. It is possible that decreasing the amount of PCBM in the active layer prevents the formation of a truly bicontinuous interpenetrating network, thus facilitating charge recombination. In a similar case, van Duren et al. [46] reported that the current density of MDMO-PPV/PCBM cells peaks at a 75–80 wt% fullerene concentration (1:4 ratio) in spite of the theoretical percolation value of 25 wt%.

The nature of the V_{oc} has been the subject of recent discussions [3,11,49]. Roughly, the V_{oc} is directly related to the energy difference between the HOMO of the donor and the LUMO of the acceptor [3,50]. Here the V_{oc} of the devices consisting of 1:4, PProDOT(Hx)₂:PCBM was found to be ~ 0.3 V, while analogous MDMO-PPV devices are found to give a V_{oc} of ~ 0.8 V [13]. The fact that the HOMO of MDMO-PPV is approximately 0.3 eV lower in energy than that of PProDOT(Hx)₂ would seem to qualitatively explain the larger V_{oc} observed for MDMO-PPV. We also found that the V_{oc} response in the PProDOT(Hx)₂:PCBM solar cells is similar to that of the MDMO-PPV/PCBM devices in response to added PCBM [46]. For PProDOT(Hx)₂, addition of 1 wt equivalent of PCBM dropped the V_{oc} from 0.560 V (from the pristine polymer device) to 0.320 V. This is similar to the V_{oc} reduction in the MDMO-PPV devices from 1.4 V for pure MDMO-PPV to ~ 0.9 V for the 1:1 polymer/PCBM blend. Further increasing the concentration of PCBM drops the V_{oc} to a range of 0.270–0.290 V. For our devices, in addition to varying the PCBM concentration, the metal contacts were changed from LiF/Al to Ca/Al. However, this also failed to increase the overall efficiency of the device and the V_{oc} did not notably improve. Varying the concentration of PCBM or changing the metal contacts did not appreciably affect the FF either.

A post-production treatment of some PV devices has been shown to enhance their activity [48]. However, several post-production conditions did not show any improvements of the 1:4 blend PV devices. The devices were heated at temperatures ranging from 85 to 125 °C while applying a bias of 2 or 3 V (see Section 2) before exposing them to white-light illumination.

3.3. Morphology of the blends by atomic force microscopy (AFM)

Understanding the morphology of the active layer can aid the understanding of the behavior of solar cells [13,44,45,51]. As previously mentioned, an intimately blended, interpenetrating network of donor–acceptor molecules is desired in order to facilitate the photoinduced charge transfer. In the case where phase separation leads to very large domains (on the order of several hundred nanometers), the formation of charge carriers can be hindered due to the lack of available interfaces at which charge transfer can occur as is limited by the exciton diffusion length of $\sim 5\text{--}10$ nm in a conjugated polymer [14]. However, it has also been postulated that thorough mixing, to the point of a continuous network, can enhance charge recombination due to the close proximity of the donor and acceptor molecules. As a result, if the domain sizes are too large or if the blend is essentially homogeneous, the overall efficiency is reduced due to a decrease in the number of charges generated [51]. An AFM study of the morphology of PProDOT(Hx)₂/PCBM blends, spin coated from CB, supports the above observations and is also consistent with previous results that correlate the performance of the solar cells to the morphology [46]. Fig. 8 shows the height images obtained by AFM for PProDOT(Hx)₂/PCBM films for three different compositions (1:2, 1:3, 1:4) spin coated from two different solvents (CB [a–c] and CF [d]) for the 1:4 blend. As can be seen in Fig. 8(a and b), PProDOT(Hx)₂/PCBM films prepared from 1:2 and 1:3 ratio from CB have rather smooth surfaces with a height scale (maximum peak to valley roughness) of 5 nm, an indication of a large interface between the donor and acceptor, potentially facilitating charge recombination. Indeed, solar cells based on these blends had poor efficiencies of 0.05 and 0.07 (for 1:2 and 1:3, respectively). The films based on a 1:4 weight ratio of PProDOT(Hx)₂:PCBM from CB (Fig. 8c) have larger phase separated domains compared to those of the 1:2 or 1:3 blends from the same solvent. With the 1:4 blend (CB), the domain size varied between 90 and 160 nm. As previously discussed, the 1:4 blend gave the best photovoltaic results, corresponding to the point where phase separation begins to occur. Furthermore, it is known that spin coating from different solvents can also change the morphology of the devices [51]. PProDOT(Hx)₂/PCBM films of 1:4 ratio from CF showed an increase in the size of the phase-separated domains ranging from 160 to 430 nm (see Fig. 8d). Surprisingly, the effects on the efficiency were not as drastic as the changes observed in the morphology. For the film cast from CF, the current density decreased by only 0.16 mA cm^{-2} , compared to the 1:4 blend spin coated from CB, and the device showed a decrease in the V_{oc} of 0.01 V, also relative to the CB cast film.

4. Conclusions

We have studied the performance of PProDOT(Hx)₂/PCBM bulk heterojunction solar cells. The polymer has a band gap of 1.9 eV, as measured by optical absorption spectroscopy and cyclic voltammetry, and interacts well in the excited state with PCBM by photoinduced charge transfer. The PL of PProDOT(Hx)₂ is significantly quenched at low concentrations of PCBM in the blend and the PIA spectra of PProDOT(Hx)₂/PCBM blends show the formation of polaronic charge carriers on the conjugated polymer, along with second-order recombination kinetics. The photocurrent spectrum covers the absorption range of PProDOT(Hx)₂, showing the photoactivity of the polymer in combination with the fullerene acceptor. Although the solar cell efficiency was rather low

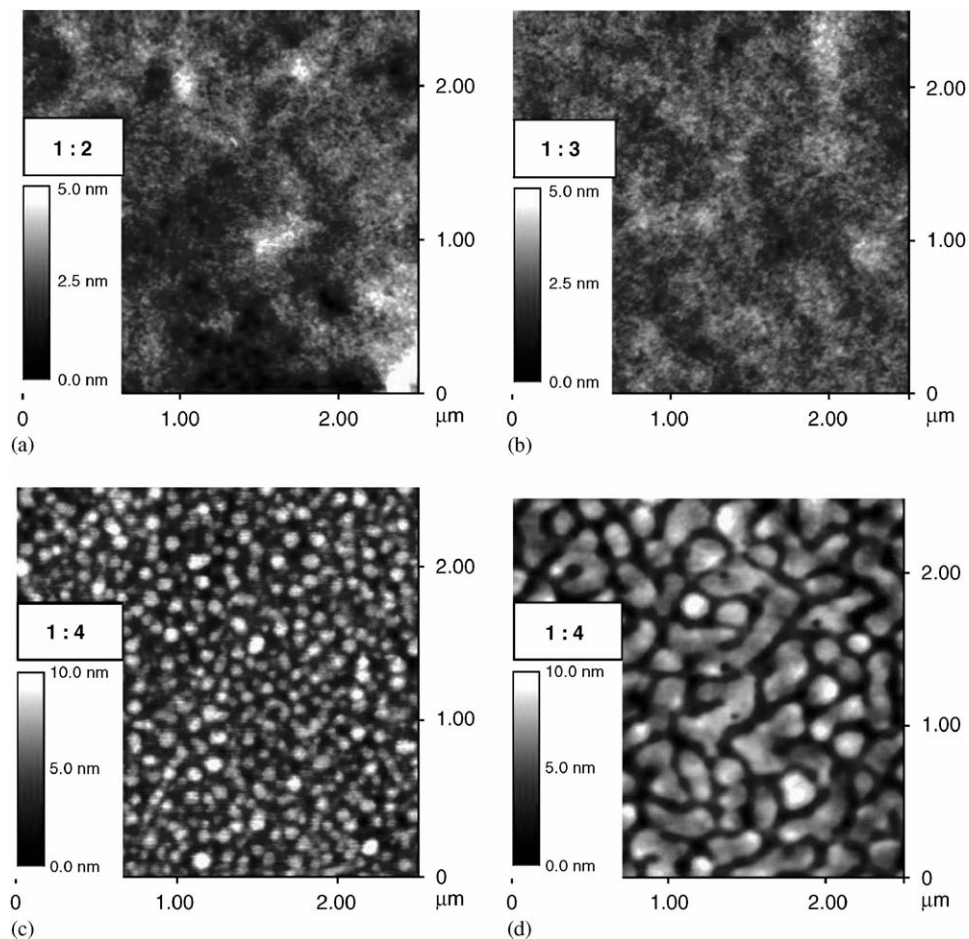


Fig. 8. AFM images showing the surface of different PProDOT(Hx)₂/PCBM blends spin coated from CB (1:2, 1:3, and 1:4; a, b, and c, respectively) and CF (1:4, d).

(0.1%), the possible application combination in electrochromic and photovoltaic devices makes PProDOT(Hx)₂ an interesting material. The feasibility of synthesizing similar polymers in industrial amounts, with multiple applications in materials science, should drive an interest to tailor similar polymers to meet the demands for solar cell development.

Acknowledgments

This work was funded by the Christian Doppler Laboratory for Plastic Solar Cells (Austria). The Air Force Office of Scientific Research (FA955-06-1-0192) funded the work at the University of Florida. LMC thanks the National Science Foundation, the Paul and Daisy Soros Fellowship, and the NSF IGERT: Materials Creation Training Program (MCTP)—(Grant no. DGE-0114443) for graduate support. SG thanks the Turkish Council of Higher Education (YÖK) for a national award scholarship.

References

- [1] N.S. Sariciftci, L. Smilowitz, A.J. Heeger, F. Wudl, *Science* 258 (1992) 1474.
- [2] (a) H. Hoppe, N.S. Sariciftci, *J. Mater. Res.* 19 (2004) 1924;
(b) *Sol. Energy Mater. Sol. Cells* 83 (2004) 2 (special issue);
(c) *MRS Bull* 30 (2005) 1 (special issue).
- [3] C.J. Brabec, *Sol. Energy Mater. Sol. Cells* 83 (2004) 273.
- [4] G. Yu, J. Gao, J.C. Hummelen, F. Wudl, A.J. Heeger, *Science* 270 (1995) 1789.
- [5] (a) C. Waldauf, P. Schilinsky, J. Hauch, C.J. Brabec, *Thin Solid Films* 451–452 (2004) 503;
(b) G. Li, V. Shrotriya, J. Huang, Y. Yao, T. Moriarty, K. Emery, Y. Yang, *Nature Mater.* 4 (2005) 864;
(c) W. Ma, C. Yang, X. Gong, K. Lee, A.J. Heeger, *Adv. Funct. Mater.* 15 (2005) 1617.
- [6] (a) C.J. Brabec, N.S. Sariciftci, J.C. Hummelen, *Adv. Funct. Mater.* 11 (2001) 15;
(b) K.M. Coakley, M.D. McGehee, *Chem. Mater.* 16 (2004) 4533.
- [7] B. Kraabel, J.C. Hummelen, D. Vacar, D. Moses, N.S. Sariciftci, A.J. Heeger, F. Wudl, *J. Chem. Phys.* 104 (1996) 4267.
- [8] S. Morita, A.A. Zakhidov, K. Yoshino, *Solid State Commun.* 82 (1992) 249.
- [9] M.M. Wienk, J.M. Kroon, W.J.H. Verhees, J. Knol, J.C. Hummelen, P.A. van Hal, R.A.J. Janssen, *Angew. Chem. Int. Ed.* 42 (2003) 3371.
- [10] S. Alem, R. de Bettignies, J.-M. Nunzi, M. Cariou, *Appl. Phys. Lett.* (2004) 84.
- [11] C.J. Brabec, A. Cravino, D. Meissner, N.S. Sariciftci, T. Fromherz, M.T. Rispens, L. Sanchez, J.C. Hummelen, *Adv. Funct. Mater.* 11 (2001) 374.
- [12] F.L. Zhang, A. Gadisa, O. Inganas, M. Svensson, M.R. Andersson, *Appl. Phys. Lett.* 84 (2004) 3906.
- [13] S.E. Shaheen, C.J. Brabec, N.S. Sariciftci, F. Padinger, T. Fromherz, J.C. Hummelen, *Appl. Phys. Lett.* 78 (2001) 841.
- [14] C. Winder, N.S. Sariciftci, *J. Mater. Chem.* 14 (2004) 1077.
- [15] L.M. Campos, A. Tontcheva, S. Günes, G. Sonmez, H. Neugebauer, N.S. Sariciftci, F. Wudl, *Chem. Mater.* 17 (2005) 4031.
- [16] (a) T. Jeranko, H. Tributsch, N.S. Sariciftci, J.C. Hummelen, *Sol. Energy Mater. Sol. Cells* 83 (2004) 247;
(b) F.C. Krebs, J.E. Carle, N. Cruys-Bagger, M. Andersen, M.R. Lilliedal, M.A. Hammond, S. Hvidt, *Sol. Energy Mater. Sol. Cells* 86 (2005) 499.
- [17] (a) J. Roncali, *Chem. Rev.* 97 (1997) 173;
(b) J.L. Reddinger, J.R. Reynolds, *Adv. Polym. Sci.* 145 (1999) 57.
- [18] L. Groenendaal, F. Jonas, D. Freitag, H. Pielartzik, J.R. Reynolds, *Adv. Mater.* (2000) 12.
- [19] L. Groenendaal, G. Zotti, P.-H. Aubert, S.M. Waybright, J.R. Reynolds, *Adv. Mater.* 15 (2003) 855.
- [20] A. Kumar, D.M. Welsh, M.C. Morvant, F. Piroux, K.A. Abboud, J.R. Reynolds, *Chem. Mater.* (1998) 10.
- [21] D.M. Welsh, A. Kumar, E.W. Meijer, J.R. Reynolds, *Adv. Mater.* 11 (1999) 1379.
- [22] D.M. Welsh, L.J. Kloppe, L. Madrigal, M.R. Pinto, B.C. Thompson, K.S. Schanze, K.A. Abboud, D. Powell, J.R. Reynolds, *Macromolecules* 35 (2002) 6517.
- [23] (a) B.D. Reeves, C.R.G. Greiner, A.A. Argun, A. Cipran, T.D. McCarley, J.R. Reynolds, *Macromolecules* 37 (2004) 7559;
(b) B.C. Thompson, Y.G. Kim, J.R. Reynolds, *Macromolecules* 38 (2005) 5359.
- [24] A. Cirpan, A.A. Argun, C.R.G. Grenier, B.D. Reeves, J.R. Reynolds, *J. Mater. Chem.* (2003) 13.
- [25] (a) A.J. Mozer, P. Denk, M.C. Scharber, H. Neugebauer, N.S. Sariciftci, P. Wagner, L. Lutsen, D. Vanderzande, *J. Phys. Chem. B* 108 (2004) 5235;
(b) C. Arndt, U. Zhokhavets, G. Gobsch, C. Winder, C. Lungenschmied, N.S. Sariciftci, *Thin Solid Films* 451–452 (2004) 60.
- [26] V.V. Pavlishchuk, A.W. Addison, *Inorg. Chim. Acta* 298 (2000) 97.
- [27] A.J. Bard, L.R. Faulkner, in: *Electrochemical Methods: Fundamentals and Applications*, second ed., Wiley, New York, 2001, p. 54.
- [28] Y. Li, Y. Cao, J. Gao, D. Wang, G. Yu, A.J. Heeger, *Synth. Met.* 99 (1999) 243.
- [29] M. Al-Ibrahim, H.-K. Roth, U. Zhokhavets, G. Gobsch, S. Sensfuss, *Sol. Energy Mater. Sol. Cells* 85 (2005) 13.
- [30] C. Winder, G. Matt, J.C. Hummelen, R.A.J. Janssen, N.S. Sariciftci, C.J. Brabec, *Thin Solid Films* 403–404 (2002) 373.
- [31] S.C.J. Meskers, J. Hubner, M. Oestreich, H. Bassler, *J. Phys. Chem. B* 105 (2001) 105.
- [32] M. Theander, O. Inganas, W. Mammo, T. Olinga, M. Svensson, M.R. Anderson, *J. Phys. Chem. B* 103 (1999) 7771.

- [33] K. Schmieder, M. Levitus, H. Dang, M.A. Garcia-Garibay, *J. Phys. Chem. A* 106 (2002) 1551.
- [34] M. Levitus, G. Zepeda, H. Dang, C. Godinez, T.-A.V. Khuong, K. Schmieder, M.A. Garcia-Garibay, *J. Org. Chem.* 66 (2001) 3188.
- [35] J.R. Lackowitz, *Principles of Fluorescence Spectroscopy*, Kluwer Academic/Plenum Publishers, New York, 1999.
- [36] M. Levitus, M.A. Garcia-Garibay, *J. Phys. Chem. A* 104 (2000) 8632.
- [37] J.C. Hummelen, B.W. Knight, F. LePeq, F. Wudl, J. Yao, C.L. Wilkins, *J. Org. Chem.* 60 (1995) 532.
- [38] R.A.J. Janssen, J.C. Hummelen, K. Lee, K. Pakbaz, N.S. Sariciftci, A.J. Heeger, F. Wudl, *J. Chem. Phys.* 103 (1995) 788.
- [39] C.J. Brabec, C. Winder, N.S. Sariciftci, J.C. Hummelen, A. Dhanabalan, P.A. van Hal, R.A.J. Janssen, *Adv. Funct. Mater.* 12 (2002) 709.
- [40] R.N. Marks, J.J.M. Halls, D.D.C. Bradley, R.H. Friend, A.B. Holmest, *J. Phys.: Condens. Matter* 6 (1994) 1379.
- [41] M.G. Harrison, J. Gruener, G.C.W. Spencer, *Phys. Rev. B* 55 (1997) 7831.
- [42] C. Im, W. Tiam, H. Bassler, A. Fechtenkötter, M.D. Watson, K. Mullen, *J. Chem. Phys.* 119 (2003) 3952.
- [43] O. Epshtein, G. Nakhmanovich, Y. Eichen, E. Ehrenfreund, *Phys. Rev. B* 63 (2001) 125206.
- [44] C.Y. Yang, A.J. Heeger, *Synth. Met.* 83 (1996) 85.
- [45] J. Liu, Y. Shi, Y. Yang, *Adv. Funct. Mater.* 11 (2001) 420.
- [46] J.K.J. van Duren, X. Yang, J. Loos, C.W.T. Bulle-Lieuwma, A.B. Sieval, J.C. Hummelen, R.A.J. Janssen, *Adv. Funct. Mater.* 14 (2004) 425.
- [47] C.J. Brabec, A. Cravino, D. Meissner, N.S. Sariciftci, M.T. Rispens, L. Sanchez, J.C. Hummelen, T. Fromherz, *Thin Solid Films* 403–404 (2002) 368.
- [48] F. Padinger, R. Rittberger, N.S. Sariciftci, *Adv. Funct. Mater.* 13 (2003) 85.
- [49] V.D. Mihailetschi, P.W.M. Blom, J.C. Hummelen, M.T. Rispens, *J. Appl. Phys.* 94 (2003) 6849.
- [50] A. Gadisa, M. Svensson, M.R. Anderson, O. Inganäs, *Appl. Phys. Lett.* 84 (2004) 1609.
- [51] M.T. Rispens, A. Meetsma, R. Rittberger, C.J. Brabec, N.S. Sariciftci, J.C. Hummelen, *Chem. Commun.* 17 (2003) 2116.